Supporting information for
Resonant bonding, multiband thermoelectric transport and native defects in n-type $BaBiTe_{3-x}Se_x$ (x = 0, 0.05 and 0.1)

S. Maier[1], S. Ohno[2,3], G. Yu[4], S. D. Kang[2,3], T. C. Chasapis[3], V. A. Ha[4], S. A. Miller[3], D. Berthebaud[1], M. G. Kanatzidis[5], G.-M. Rignanese[4], G. Hautier[4], G. J. Snyder[3] and F. Gascoin[1]*

[1]*Laboratoire CRISMAT UMR 6508 CNRS ENSICAEN, 6 boulevard du Maréchal Juin, 14050 Caen Cedex 04, France*

[2]*Department of Applied Physics and Materials Science, California Institute of Technology, CA 91125, USA*

[3]*Department of Materials Science and Engineering, Northwestern University, Evanston, IL 60208, USA*

[4]*Institute of Condensed Matter and Nanosciences (IMCN), Université catholique de Louvain, 1348 Louvain-la-Neuve, Belgium*

[5]*Chemistry Department, Northwestern University, Evanston, IL 60208, USA*

*Corresponding author. Tel: +33-2-31452605. Fax: +33-2-31951600.
E-mail address: franck.gascoin@ensicaen.fr (F. Gascoin).

Table of contents

I Speed of sound measurements and evaluation of ω_D and θ_D
II Energy dispersive X-ray spectroscopy (EDS)
III Extrinsic defect calculations
IV Electronic structure calculations
V COHP curves containing Ba-Te interactions
VI Thermal diffusivities

I Speed of sound measurements and evaluation of ω_D and θ_D

The longitudinal and transversal components of the speed of sound (v_L and v_T) were measured applying the pulse-echo method. A piezoelectric transducer coupled to the sample first sends the initial pulse, and then acts as receiver measuring the echoed reflections. The time delay, t_d, between subsequent reflections was determined by maximizing the cross-correlation of the two reflections as follows. If $\sigma_n(t)$ corresponds to the stress amplitude of reflection (n), then $\sum_t \sigma_n(t)\sigma_{n+1}(t-t_d)$ is maximized by varying t_d. A longitudinal transducer with a principle frequency of 20 MHz (Olympus M116-RM) and a transverse transducer at 5 MHz (Olympus V157-RM) were used with a Panametrics 5072PR pulse-receiver. A Tektronix TBS 1072B-EDU oscilloscope was used to record the waveforms.

Table I speed of sound data, debye temperatures and frequencies of $BaBiTe_3$ and $BaBiSe_3$

	$BaBiTe_3$	**$BaBiSe_3$**
v_s (m/s)	1820	1977
v_T (m/s)	1462	1535
v_L (m/s)	2536	2863
θ_D (K)	147	164
ω_D (rad/s)	$1.92 \cdot 10^{13}$	$2.15 \cdot 10^{13}$

II Energy dispersive X-ray spectroscopy (EDS)

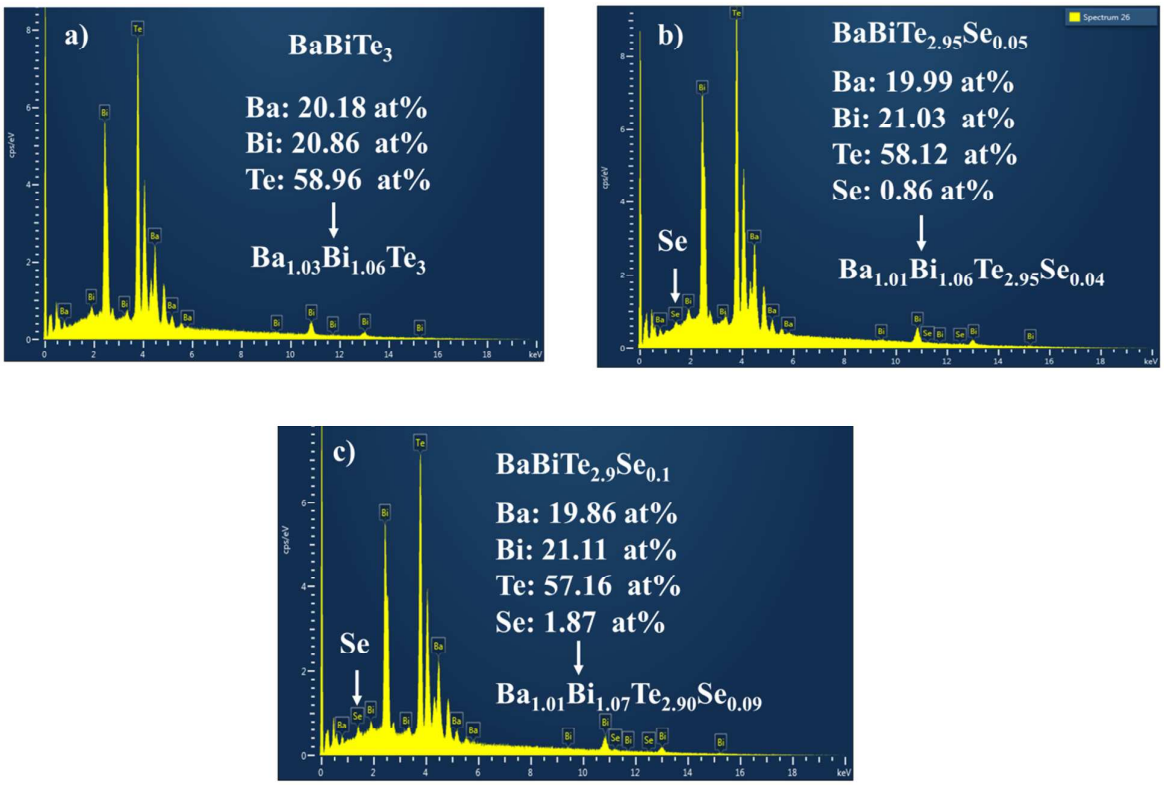

Figure S1 Experimental EDS spectra of all characterized samples with the corresponding nominal and experimental compositions.

III Extrinsic defect calculations

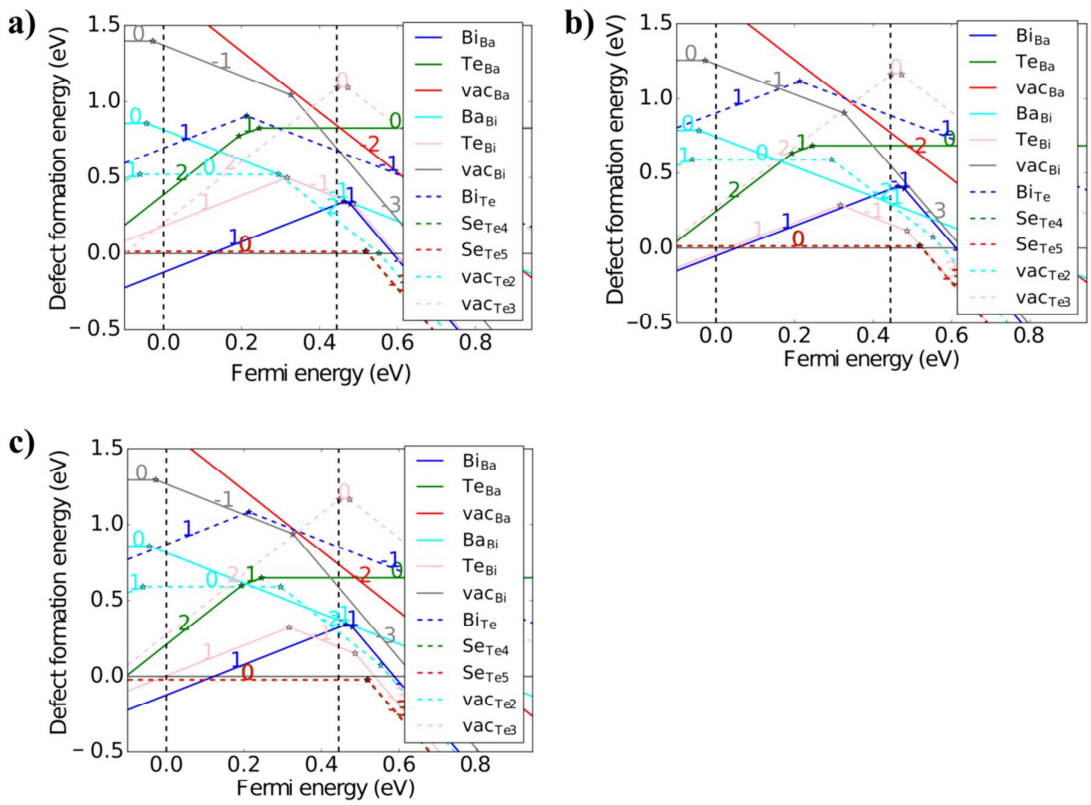

Figure S2 Extrinsic defect calculations showing an equally low defect formation energy of 0 for Se_{Te4} and Se_{Te5} defects. a)-c) correspond to three different regions of the Ba-Bi-Te-Se phase diagram.

IV Electronic structure calculations

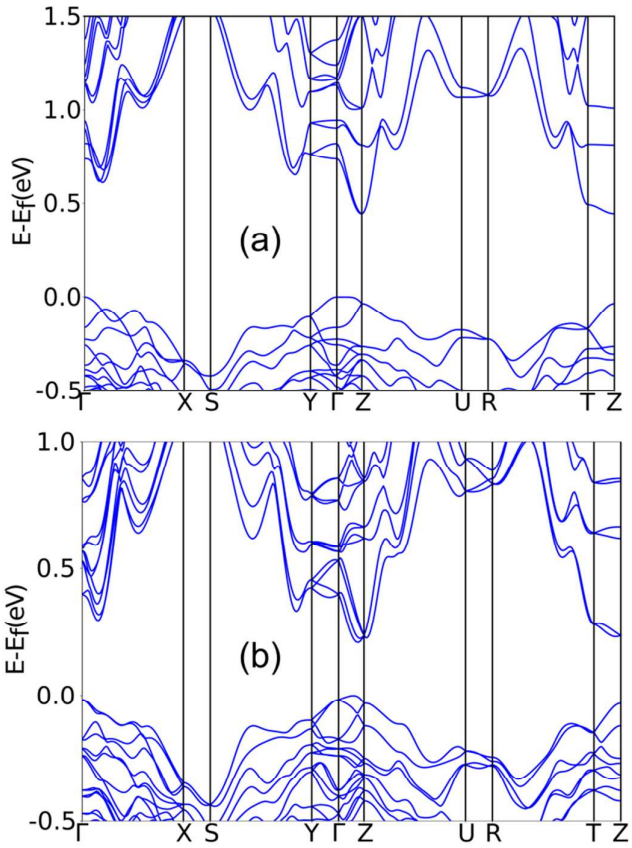

Figure S3 Electronic structure of $BaBiTe_3$ a) without spin-orbit coupling (SOC) b) with SOC ; the results show that SOC decreases the band gap, but does not dramatically change the overall bandstructure.

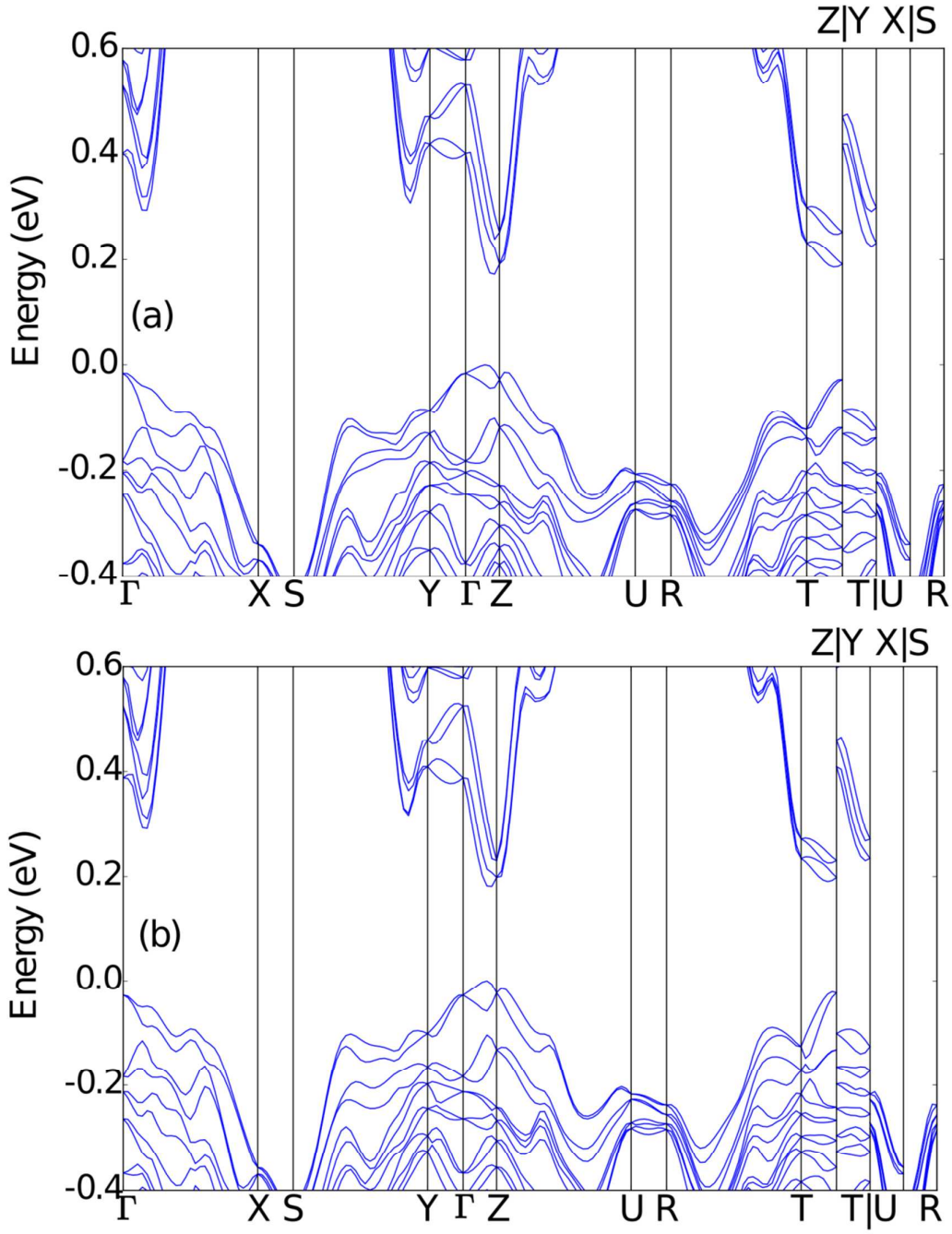

Figure S4 Electronic structure of $BaBiTe_{2.875}Se_{0.125}$; a) Se substitution on Te4 site, b) Se substitution on Te5 site. This image demonstrates that the three electron pockets are also present in Se substituted variants of $BaBiTe_3$.

V COHP curves containing Ba-Te interactions

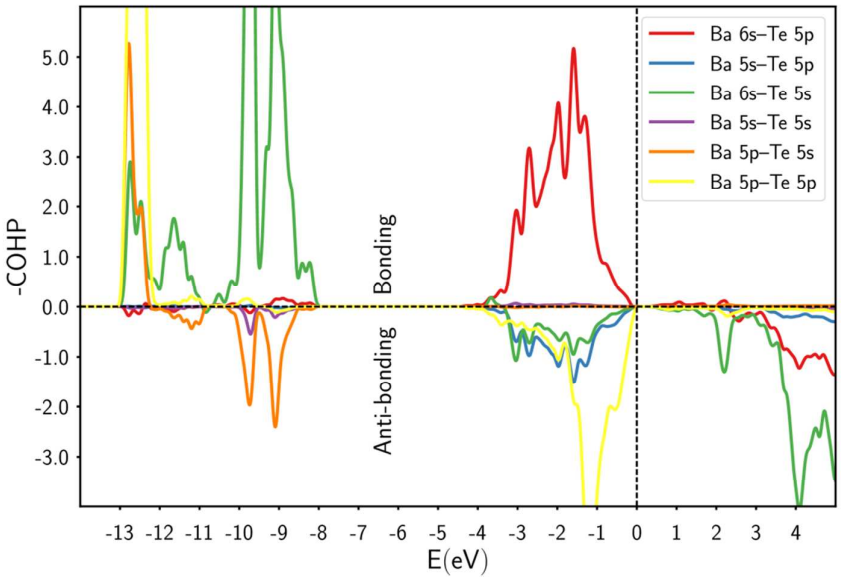

Figure S5 COHP curves showing all Ba-Te interactions. This graph shows significant contributions of Ba6s-Te5p bonding and Ba5p-Te5p antibonding states to the valence band edge, i.e. the ionic part of the crystal structure of $BaBiTe_3$ can be expected to play a significant role to the electronic transport in $BaBiTe_3$.

VI Thermal diffusivities

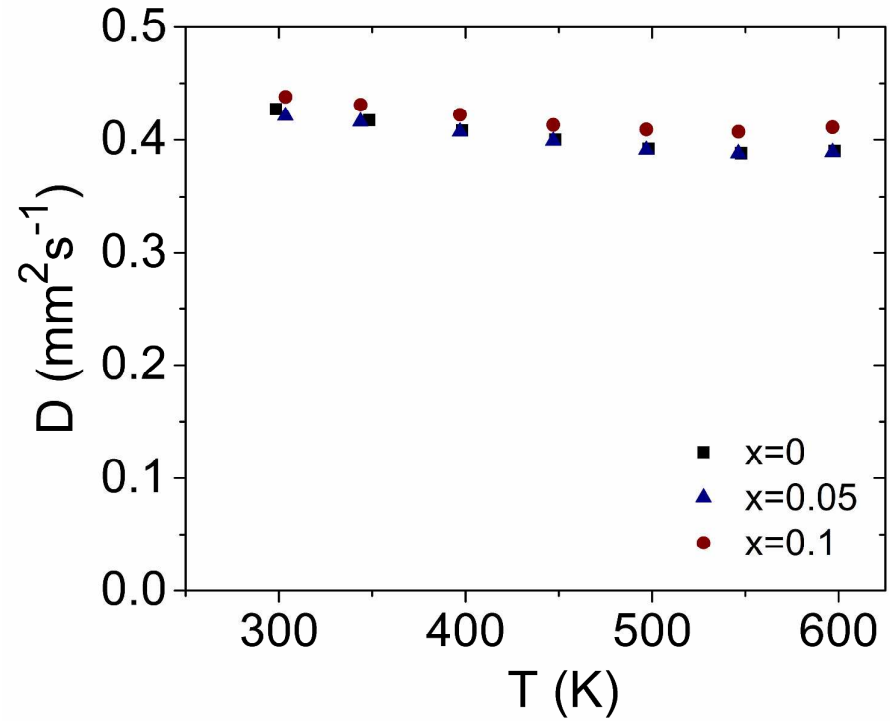

Figure S6 Thermal diffusivities of black: $BaBiTe_3$, blue: $BaBiTe_{2.95}Se_{0.05}$ and red: $BaBiTe_{2.9}Se_{0.1}$